

UNCLASSIFIED

AD 4 3 8 9 4 7

DEFENSE DOCUMENTATION CENTER

FOR

SCIENTIFIC AND TECHNICAL INFORMATION

CAMERON STATION, ALEXANDRIA, VIRGINIA



UNCLASSIFIED

NOTICE: When government or other drawings, specifications or other data are used for any purpose other than in connection with a definitely related government procurement operation, the U. S. Government thereby incurs no responsibility, nor any obligation whatsoever; and the fact that the Government may have formulated, furnished, or in any way supplied the said drawings, specifications, or other data is not to be regarded by implication or otherwise as in any manner licensing the holder or any other person or corporation, or conveying any rights or permission to manufacture, use or sell any patented invention that may in any way be related thereto.

64 13

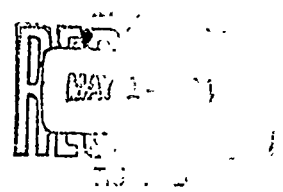
AEDC-TDR-64-49

438947



**OBSERVATIONS OF HYPERVELOCITY IMPACT
OF TRANSPARENT PLASTIC TARGETS**

By



Ray Kinslow

von Kármán Gas Dynamics Facility
ARO, Inc.

CATALOGED BY DDC

438947

TECHNICAL DOCUMENTARY REPORT NO. AEDC-TDR-64-49

May 1964

Program Element 62405364/8871, Task 887101

(Prepared under Contract No. AF 40(600)-1000 by ARO, Inc.,
contract operator of AEDC, Arnold Air Force Station, Tenn.)

**ARNOLD ENGINEERING DEVELOPMENT CENTER
AIR FORCE SYSTEMS COMMAND
UNITED STATES AIR FORCE**

NOTICES

Qualified requesters may obtain copies of this report from DDC, Cameron Station, Alexandria, Va. Orders will be expedited if placed through the librarian or other staff member designated to request and receive documents from DDC.

When Government drawings, specifications or other data are used for any purpose other than in connection with a definitely related Government procurement operation, the United States Government thereby incurs no responsibility nor any obligation whatsoever; and the fact that the Government may have formulated, furnished, or in any way supplied the said drawings, specifications, or other data, is not to be regarded by implication or otherwise as in any manner licensing the holder or any other person or corporation, or conveying any rights or permission to manufacture, use, or sell any patented invention that may in any way be related thereto.

OBSERVATIONS OF HYPERVELOCITY IMPACT
OF TRANSPARENT PLASTIC TARGETS

By

Ray Kinslow*

von Kármán Gas Dynamics Facility

ARO, Inc.

a subsidiary of Sverdrup and Parcel, Inc.

May 1964

ARO Project No. VS2401

*Chairman, Department of Engineering Science, Tennessee Poly-
technic Institute, Cookeville, Tennessee, and Consultant, ARO, Inc.

ABSTRACT

Targets of transparent plastic have been impacted with projectiles at velocities up to 25,000 ft/sec. Photographs made of approximately 6×10^5 frames per second show the projectile, luminous flash, crater formation, and shock waves in the target. The propagation of the waves and their reflections, and the fractures they produce, are analyzed. Spalling near the rear surface of the target is seen as the shock is reflected as a tensile wave. Studies of laminated targets show transmission and reflection of shock waves at each interface together with details of the complex fracture patterns. These are also analyzed. A theory of fracture is presented which predicts that the fracture of Plexiglas or Lucite is time-dependent and is affected by the target's rear surface and the target temperature. It is shown that most of the effects of hypervelocity impact can be simulated by the use of explosives placed in small holes in the target. This not only results in savings of both time and cost, but also in crater location with an accuracy that would be impossible to the use of a gun. These studies of transparent targets give insight into the nature of cratering and fracture by hypervelocity impact.

PUBLICATION REVIEW

This report has been reviewed and publication is approved.

Hans K. Doetsch
H. K. Doetsch
Technical Advisor
DCS/Research

Donald R. Eastman
Donald R. Eastman, Jr.
DCS/Research

CONTENTS

	<u>Page</u>
ABSTRACT	iii
1.0 INTRODUCTION	1
2.0 BRIEF DESCRIPTION OF MATERIAL FRACTURE	1
3.0 INITIAL STAGE OF IMPACT	2
4.0 FRACTURES INDUCED BY IMPACT	2
5.0 SHOCK PROPAGATION AND REFLECTION	5
6.0 FRACTURE OF LAMINATED TARGETS	5
7.0 SIMULATION OF IMPACT CONDITIONS BY USE OF EXPLOSIVES	7
8.0 EFFECT OF TARGET SURFACE	8
9.0 REFLECTIONS FROM CURVED SURFACES	8
10.0 EFFECT OF TARGET TEMPERATURE	9
11.0 CONCLUSIONS	10
REFERENCES	11

ILLUSTRATIONS

Figure

1. Hypervelocity Impact of Transparent Target	13
2. Fractures Produced by Hypervelocity Impact	14
3. Fractures Produced by Exploding Blasting Caps	15
4. Fracture Formation (T99)	16
5. Stress Waves and Fracture (T99)	17
6. Sector of Fractured Target (T99)	18
7. Fracture Formation (206)	19
8. Section of Fractured Target	20
9. Residual Stresses in Target	21
10. Pulse Velocity for Various Impact Velocities	22
11. Development of Radial Tensile Stress Caused by Reflected Pulse	23
12. Mechanics of Fracture Caused by Reflected Pulse	24
13. Photograph of Reflected Pulse Front Moving Ahead of the Fracture	25

<u>Figure</u>	<u>Page</u>
14. Example of Secondary Fracture	26
15. Impact of Laminated Target	27
16. Fracture Formation in Laminated Target (T311)	28
17. Stress Wave and Fracture of Laminated Target (T311).	29
18. Effect of Target Thickness	30
19. Fractures in Targets Having Small Lateral Dimensions	31
20. Mechanics of Fracturing	32
21. Fractures in a Triangular Target	33
22. Fractures in Targets of Various Geometrical Shapes	34
23. Effect of Rear Surface Conditions	35
24. Fractures Caused by Reflections from Curved Surfaces	36
25. Fracture Along Axes of Long Cylindrical Rods	37
26. Fractures Along Axis and at End of a Cylindrical Rod	38
27. Transverse Fracture of a Cylindrical Rod	39
28. Fractures in a Short Cylinder	40
29. Sections of Fractured Cylinders	41
30. Effect of Target Temperature	42

1.0 INTRODUCTION

One of the difficult problems presented by flight through the environment of space is the protection of spacecraft against disastrous impact damage by meteoroids and projectiles. Considerable research is being directed to defining and reducing this hazard. Speeds of interplanetary debris are estimated to average about 50,000 ft/sec and to go as high as 200,000 ft/sec (Refs. 1 and 2). The pressures produced by impacts at such velocities may reach several million pounds per square inch. Little is known about the properties of materials under these conditions. Observations of the effects of hypervelocity impact upon targets of transparent materials such as Lucite* or Plexiglas* contribute to an understanding of the physical nature of the mechanism of this phenomenon. The high-velocity impact test results were obtained in the impact ranges at the Arnold Engineering Development Center (AEDC), Air Force Systems Command (AFSC). Most of the tests simulating impact conditions by explosions were carried out at the Tennessee Polytechnic Institute.

2.0 BRIEF DESCRIPTION OF MATERIAL FRACTURE

A simplified description of the effects resulting from high-velocity impact of plastic targets may be divided into the following stages, each of which is analyzed in greater detail later in this study.

1. The projectile is imbedded only slightly in the target material and then appears to explode, causing the pressure applied to the target face to rise very rapidly to an extremely high value.
2. A spherical shock wave is formed within the target, centered upon the point of first contact. Crushing and melting of the target material results. The melted region is approximately hemispherical. Some of the material near the surface is ejected, producing a rough, irregularly shaped crater.
3. The spherical shock wave decays very rapidly into a compressive elastic pulse, the strength of which decreases as it continues to move through the target.

*Acrylic (methyl methacrylate) resin manufactured under the trade names Lucite (E. I. du Pont de Nemours Co.) and Plexiglas (Rohm and Haas Co.).

Manuscript received February 1964.

4. A large number of needle-like fractures are formed, radiating outward from the hemispherical region of crushed and melted material. The melted portion of the target solidifies and contracts, producing radial tensile stresses and fracture around this region.
5. If the elastic compression pulse reaches a free surface (such as the rear face of the target), it will be reflected as a tensile pulse. If the magnitude of this reflected tensile pulse is equal to or greater than the fracture strength of the target material, fractures will occur. If the pulse is of sufficient magnitude, the portion of the target between the fracture produced by the reflected wave and the rear face of the target may shatter; and in some cases this portion may become detached from the target and fly off at a high velocity. Fractures may also be formed if two or more reflected waves meet and the sum of their amplitudes equals or exceeds the target strength.

Most of the stages outlined above may be observed in Fig. 1 which shows frames selected from a film made of a 30-cal x 0.15-in. Lexan projectile impacting a 2-in. target at a velocity of 21,800 ft/sec. These photographs are silhouettes made with a Beckman & Whitley camera (model 192) capable of a speed of 1.4 million frames per second. The target was backlighted by means of a high-intensity xenon flash.

3.0 INITIAL STAGE OF IMPACT

The fact that the projectile behaves explosively after it is imbedded only slightly in the target is demonstrated in Figs. 2 and 3. The photographs in Fig. 2 are of plastic targets which have been impacted with projectiles having velocities ranging from 11,000 to 17,600 ft/sec. Those shown in Fig. 3 are blocks of plastic which have been fractured by the exploding of No. 8 Hercules blasting caps. These caps were inserted in holes drilled to various depths in the plastic after 1/4-in. aluminum hemispheres were placed in each hole. It is difficult to distinguish between the fractures produced by impact and those produced by explosives.

4.0 FRACTURES INDUCED BY IMPACT

The fracture of the target shown in Fig. 1 was formed at a very irregular rate. Figure 4 shows this in detail. The camera speed for

this test was 5.8×10^5 frames per second. The number which identifies each contour denotes the frame number; the contour itself indicates the limit of the fracture seen in that frame. It should be kept in mind that these limits were determined from silhouettes and, therefore, may not represent the actual fracture limits. Through frame 3, the fracture is hemispherical in shape. In frame 5 the fracture becomes wider at the target face, and this continues through the frame 11. These are probably the needle-like fractures which radiate out from the point of impact. The fractures along the axis then cease, and apparently the radial fractures elongate and move inward toward the axis through frame 17. They continue to elongate but at a much slower rate. Figure 5 shows the fracture location along the axis as a function of time. Photographs of a sector of this target are shown in Fig. 6. The clear portion is that which apparently was melted and then resolidified. Figure 7 shows the fracture formation in a target which was impacted by a projectile at a velocity of 14,000 ft/sec.

The photograph of a thin section cut from the center of a target is shown in Fig. 8. The impacting velocity here was 17,600 ft/sec. The various stages of the fracture are clearly seen. The fine radial fractures are probably caused by the strong tangential tensile stress which has been shown to accompany the high radial compressive forces (Ref. 3). A photoelastic analysis of the clear hemispherical portion of the target shows it to be in a state of high residual stress. Figure 9 shows this stress pattern and the 0-, 15-, 30-, and 45-deg isoclinics. This seems to confirm the theory that this portion of the target has melted and resolidified. The contraction during resolidification produced cracks around this region.

It has been shown that the velocity of crack propagation in this material is about 5,000 ft/sec (Ref. 4). As this is approximately one-half of the velocity of the stress pulse, cracks initiated by the leading edge of the pulse are unable to spread more than a short distance before they are overtaken by the pulse's trailing edge and the stress is removed, thereby arresting crack formation.

5.0 SHOCK PROPAGATION AND REFLECTION

Referring again to Fig. 5 for the case of a 30-cal Lexan projectile impacting a 2-in. Lucite target at 21,800 ft/sec, it is seen that the shock becomes detached from the expanding crater approximately one microsecond (μ sec) after impact. At that time its velocity is approximately 17,000 ft/sec and the pressure at the shock front is about

90 kilobars (kb) (Ref. 5). This spherical shock rapidly decays into an elastic wave, the velocity approaching a value of 10,900 ft/sec after about 3 μ sec. This wave velocity is independent of the projectile velocity, as may be seen in Fig. 10, but depends only upon the properties of the target material.

As this elastic pulse travels through the target, its stress amplitude attenuates at a rate inversely proportional to its radius (Ref. 3).

Upon reaching the rear surface of the target, the compression wave is reflected as a tensile wave. Figure 11 illustrates the development of this radial tensile stress when a compression pulse of arbitrary shape is reflected from a free surface. The resultant stress at any point during reflection is obtained by adding the stresses caused by the incident and reflected pulses. At (a) the pulse is approaching the free surface and reaches the surface at (b). Part of the pulse has been reflected at (c), but the tension is very small. The value of the tensile stress continues to increase, and at (g) one-half of the pulse has been reflected and the stress is entirely tension. At (l) the reflection is complete. Except for attenuation, the reflected tensile pulse is of the same form as the incident compression pulse.

Figure 12 shows the fracture formation when the magnitude of the reflected pulse is greater than the tensile strength of the target. The pulse shown in (a) through (e) is the same as in Fig. 11. At (f) the tensile stress reaches the critical value necessary to produce fracture. For Lucite this value has been estimated to be about 1 kb (Ref. 6). At (g) the fracture occurs approximately 1 μ sec after the critical stress is reached. This is not in agreement with observations of other investigators who report that there is no time delay between the attainment of the critical stress and the fracture of the material (Ref. 6). Figure 5 shows that the wave front has passed before fracture occurs, and this is pictured in Fig. 13. (It will be pointed out later that the formation of additional fractures which form under certain conditions would be difficult to explain if there were no time delay between the attainment of the critical stress and the fracture.) At (h) in Fig. 12 the fracture follows about 1 μ sec behind the tensile peak. The portion of the pulse trapped between the fracture and the rear surface is reflected from the fracture. In (i) and (j) the fracture continues to follow the tensile pulse. The trapped portion is now a compression pulse. At (k) the tensile pulse has attenuated in magnitude to less than the critical stress and the fracture ceases to form. This pulse continues through the target until it reaches another free surface (from which it will be reflected as a compression pulse). It is possible that this pulse may intersect another tensile pulse, and although neither is of sufficient magnitude to produce fracture their

sum may exceed the tensile strength of the material. Fractures formed in this manner will be pointed out later. It has been shown that a pressure wave is probably followed by tensile components (Ref. 3). In this case the reflected tensile pulse may combine with the forward moving tensile portion of the incident wave to create a stress greater than the material strength. This is probably the explanation of the fracture indicated by the arrow in Fig. 14. The trapped pulse continues to oscillate between the fracture and the rear surface as shown in (l) and (m) of Fig. 12. Although its magnitude is decreasing, another fracture is sometimes formed as shown in (n), and this is probably attributable to fatigue of the material.

6.0 FRACTURE OF LAMINATED TARGETS

It has been observed that laminated metal targets offer more resistance to fracture from hypervelocity impacts than do solid targets of the same material. In order to obtain information concerning fracture in these targets, photographs were made of a 30-cal Lexan projectile impacting a laminated Lucite target. The target was constructed of three sheets of 0.75-in. plastic. A thin coating of oil was smeared on each surface, and the three pieces were bolted together at their corners. The projectile had a velocity of 21,100 ft/sec, and the film was exposed at a rate of 5.9×10^5 frames per second. Selected frames are shown in Fig. 15. Both the incident and reflected pressure waves, as well as the fractures, can be seen. Details of the fracture formation are shown in Fig. 16. During the early stages, the fracture of the first sheet resembles that for solid targets (Figs. 4 and 7), but the trapped energy produces a final fracture which is much greater in the lateral direction. Figure 17 shows a plot of the observed shock and fracture propagation along the axis of the target. The letters at the top of the graph correspond to the photographs in Fig. 15.

Several interesting observations may be made from Fig. 17. When compared with Fig. 5, it is seen that the two are very similar during the early stages. The shock detaches itself after about 1μ sec and decays into an elastic wave at a distance of about 0.75 in. within the target after about 5μ sec. The initial fracture rate is about the same in both solid and laminated targets; however, the fracture does not cross the first lamination, and the needle-like radial fractures which are so prominent in the solid target are confined to the first sheet of the laminated target.

The pressure pulse continues through the target at a velocity of 10,500 ft/sec. No change in velocity can be detected as the pulse crosses

a lamination. Reflections are seen to occur at the second lamination and from the rear surface. These reflected tensile waves have velocities of 8,000 ft/sec. The decrease in wave velocity upon being reflected is probably caused by a decrease of Young's modulus of the material because of an increase in its temperature.

Fractures are formed by the reflected waves just as they are formed in solid targets. These fractures become much more complex in form, however, than do those in solid targets, as evident in Fig. 17. The explanation of the mechanism involved in the formation of these more complicated fractures is theoretical and is based upon a study of these experimental impacts. It is probably not accurate in all details. The dashed lines shown in Fig. 17 do not represent observed shocks but indicate only those which might be expected and which would account for the very complex nature of the fracturing.

At about 11μ sec, the reflection from the second lamination has increased in amplitude to the critical fracture strength of the material and a fracture begins to form. A portion of this wave continues as a reflected tensile pulse and is again reflected from the first lamination at about 17μ sec as a compression pulse. It reaches the fracture at 24μ sec. It is then again reflected as a tensile pulse, causing additional fracture as shown. In the meantime, a portion of the original reflected tensile wave was trapped between the second lamination and the fracture which started at about 11μ sec and was reflected rearward from the fracture as a compression pulse. Upon again reaching the second lamination, a portion continued in the forward direction through the third sheet of plastic. A portion of this pulse was reflected from the lamination as a tensile pulse back to the second layer of the plastic. This pulse apparently contributed to the fracture that began to occur at 15μ sec.

Returning now to the main wave as it proceeds through the target, it is seen that it reached the rear surface (a little after 15μ sec) from which it is reflected as a tensile wave, building up to the value of the fracture strength at about 18μ sec. As the fracture is formed, the tail of the pulse is reflected toward the rear surface as a compression pulse, reflecting from the rear free surface at 22μ sec and producing the fracture nearest the rear of the target.

Meanwhile, the main wave was being followed by the reflected wave which crossed the second lamination at 13μ sec. This compression wave reached the fracture being formed at 20μ sec and was again reflected as a tensile pulse, producing the third fracture in this rear layer of plastic.

At about 23μ sec, five of the fractures have merged into two along the axis of the target; however, their separate identities may still be observed in photograph G in Fig. 15.

At 31μ sec, the fracture may be seen breaking through the rear of the target. This target was completely destroyed.

7.0 SIMULATION OF IMPACT CONDITIONS BY THE USE OF EXPLOSIVES

The exact conditions of hypervelocity impact cannot be duplicated in all details by the use of explosives. Because of the savings in both time and cost, however, this simulation method is very useful in making preliminary studies. Another advantage is that the accuracy restriction involved in impinging a projectile upon a target at the desired impact point is no problem.

Photographs of targets which have been fractured by the firing of blasting caps are shown in Fig. 18. These are interesting since the explosions were identical for all three, the only difference being the target thickness (1.00, 1.25, and 1.50 in.). The fracture produced by the reflected tensile wave is barely seen in the 1.50-in. target. As this threshold of fracture is found to occur at a distance of 0.3 in. from the rear surface, it indicates that the length of the stress pulse is twice this distance, or 0.6 in. This conclusion presumes that the stress amplitude at the leading edge is not exceeded by stress amplitudes elsewhere in the pulse. If the fracture strength of 1 kb (Ref. 6) were correct, this indicates that this explosion (E-94 du Pont blasting cap inserted in a 1/4- x 1/4-in. cylindrical hole) produces a stress pulse having an amplitude of 1 kb and a length of 0.6 in. when the wave front is 1.8 in. (1.5-in. target thickness plus 0.3-in. reflection distance) from the front surface of the target.

If the target does not have large lateral dimensions, so many fractures are caused by internal reflections that the result will be confusing. Figure 19 shows two views of a 4- x 4- x 2-in. Lucite block that was fractured by exploding a cap in the center of one of the 4- x 4-in. faces. These fractures are very helpful in studying the nature of shock geometry or "optics". No attempt will be made to explain the formation of all the fractures, but a few of the more common ones which occur in a rectangular block are isolated and shown in Fig. 20. In A, the fracture near the rear surface produced by the reflected tensile wave is shown. The fractures shown in B are formed in a manner similar to that in A, by reflection of tensile waves from the four sides. Those shown in C and D are produced by the combination of the tensile pulses reflected from two surfaces. As the waves are reflected from three intersecting surfaces, momentum is trapped at the corners of the block, producing the fractures shown in E. (The

corners usually fly off at high velocity.) Fractures located at the mid-point of the edges of the block are usually formed as shown in Fig. 20. The mechanism involved in producing these mid-edge fractures is not clear to the author. Their appearance is not the same as that of the other fractures described. This type of fracture is more clearly seen in Fig. 21. This target was approximately one-half of a 4- x 4- x 2-in. block. The explosion was placed at the center of the hypotenuse. Most of the other fractures shown in Fig. 20 may also be seen in this target. In addition to the fractures produced by reflected tensile waves, fan-like fractures radiating out from the crater are often seen if the dimensions of the target are small. These usually extend toward the sides or toward the corners of the block.

Five blocks of various geometrical shapes are shown in Fig. 22. These were designed so that all plane surfaces were of equal distance from the point of the explosion. This provided a means for observing the relative strength of the shock in various directions. The explosions were identical for the five targets.

8.0 EFFECT OF TARGET SURFACE

As much of the damage to a material is caused by the shock reflection from the rear surface, it would be helpful if the rear surface could be designed so that the wave would be dispersed upon reflection, thus reducing the extent of the damage. In order to learn something of this possibility, three surface conditions were investigated. The target shown in Fig. 23-A had small V-shaped grooves cut in its rear surface. The form of the fracture was considerably different from those produced by shock reflection from a smooth surface, and cracks were formed at the root of each V. The block shown in Fig. 23-B also had V-shaped grooves in the rear surface, but they were larger than those shown in the previous figure. The fracture produced by the reflected pulse was concentrated as shown. Fractures were also formed at the bases of the V's. Except at the corners, none of the target surface became detached. The target shown in Fig. 23-C had semi-circular grooves in its rear surface. Although the explosion was identical to the two previous ones, considerable material was broken loose from the surface. The fan-like fractures described previously may be seen in these targets. Their exact cause is not known, but they do not appear in targets having large lateral dimensions.

9.0 REFLECTIONS FROM CURVED SURFACES

Pressure waves are reflected from curved surfaces in a manner similar to light rays. For irrotational waves of dilatation the angles of

incidence and reflections of the longitudinal components are equal (Ref. 7). The targets shown in Fig. 24 are 2.5-in. -diam cylinders with various amounts of material removed from one side. Some of the fractures appear very odd and complicated; however, they may be easily explained by the principles of geometric optics.

If a blasting cap is exploded at the center of one end of a long cylindrical rod, the pressure wave will be reflected from the sides of the rod. All of the reflected "rays" will meet along the axis of the rod, producing very high tensile stresses. The pulse strength will attenuate at a rate inversely proportional to the distance to the wave front, and the ratio of the amplitudes of the reflected and incident waves is a function of both the angle of reflection and the material properties. One would expect, therefore, that the variation in stress along the axis of the rod might be very irregular. This fracture along the axis may be seen in the photographs of three rods having diameters of 1.25 in. shown in Fig. 25. If the rods are short, tensile waves will be reflected from the end as well as from the side, resulting in multiple fractures as may be seen in Fig. 26. In some cases, the fracture may extend entirely across the rod, breaking off the end as shown in Fig. 27. If larger and shorter cylinders are used as targets, more fractures are formed. Figure 28 shows fractures in a 2.5-in. -diam cylinder. Still shorter cylinders appeared to be completely shattered internally. When these shorter cylinders (2.5 in. in diameter by 1.5 in. long) were sectioned and polished, the appearances were as shown in Fig. 29, where the individual fractures can be observed. These include the needle-like fractures radiating out from the point of the explosion, the clear portion which had melted and resolidified, the fractures caused by the reflection of tensile waves from the end, similar fractures around the sides caused by reflections from the cylindrical surface, and, in the longer cylinder, the fracture along the axis. There is also seen a conical fracture in each, caused by the addition of waves reflected from the side and end. The tangent of the angle made by an element of this cone and the axis should be equal to the ratio of the cylinder's length to radius. This is found to be true.

10.0 EFFECT OF TARGET TEMPERATURE

There will be great variations in the surface temperature of a spacecraft. As the properties of material are functions of temperature, it would be expected that the damage from hypervelocity impact would also vary, depending upon the temperature. A knowledge of the way that fractures in plastic depend upon temperature and material properties might be useful. In Fig. 30 are shown two blocks of Lucite which have

been subjected to identical explosions. The blocks were the same except for their temperature. The block shown in Fig. 30-A was at approximately 0°C, and the one in Fig. 30-B was at 70°C. The result of heating the target is apparent; fractures of all types are either reduced substantially or entirely eliminated.

11.0 CONCLUSIONS

It is hoped that the observations reported in this study will add to the understanding of the mechanics of fracture resulting from hypervelocity impact. This has been largely a qualitative analysis. A quantitative study is required to further enhance an understanding of the effects identified here, and further work is also required to identify the degree of impact similitude which may be possible by the blasting cap technique.

Several specific conclusions of some importance can be drawn from the work reported here. These conclusions are of a qualitative sort, and they are summarized below:

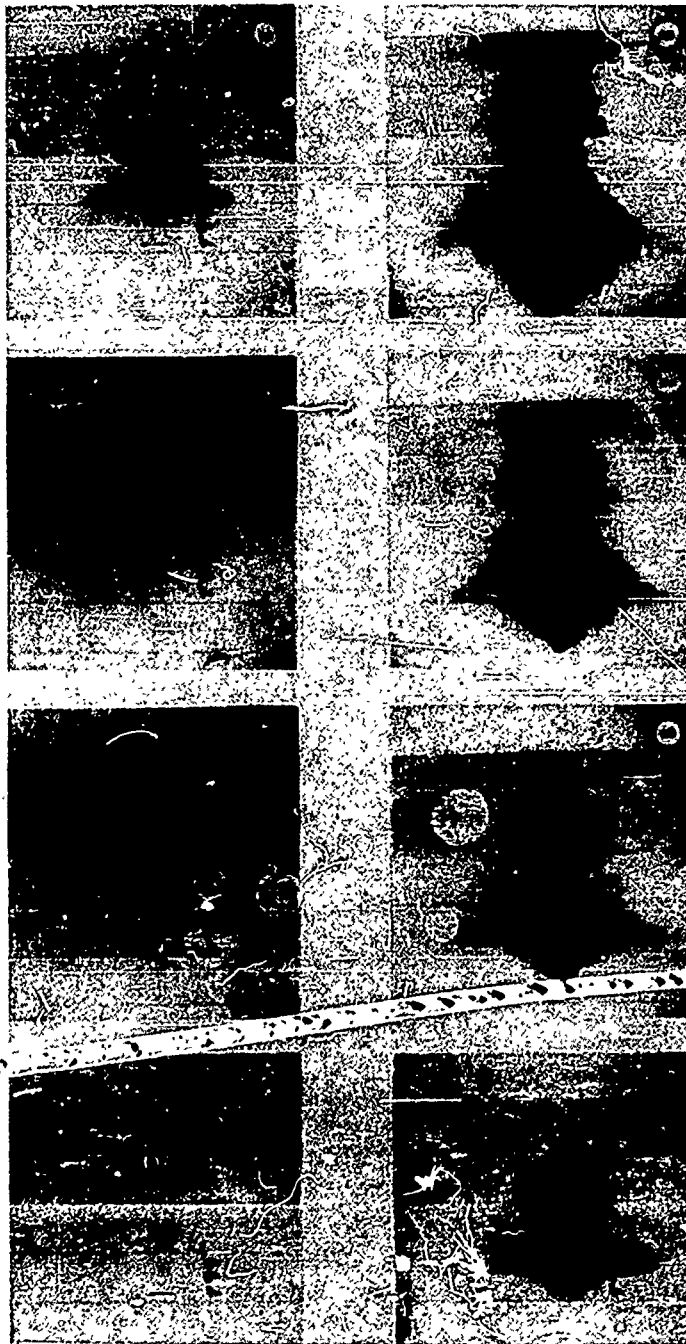
1. An impacting hypervelocity projectile behaves explosively shortly after it imbeds itself within plastic target material, and many of the effects of hypervelocity impact can be simulated by the use of explosive charges.
2. The locations of many of the fractures formed in plastic targets of uncomplicated shape can be predicted by simple principles of geometric optics.
3. Fractures arising as a result of tensile failures within plastic target materials follow the establishment of critical stress levels by a finite time delay of the order of 1 μ sec.
4. The study of laminated transparent targets offers an excellent means of observing the transmission and reflection of the stress waves. By using laminations having different properties, the observed results can be compared with theoretical studies.
5. Heating of plastic targets to temperatures near 70°C before impinging hypervelocity projectiles substantially reduces the damage they sustain.
6. The pulse length of the forcing function produced by an impacting projectile of particular mass and velocity (or by a particular explosive charge) can be simply determined.

Target thickness is adjusted until the threshold is reached at which the first plane fracture, parallel to the rear surface of the target, just occurs. The distance separating this fracture from the rear surface may then be taken as half the pulse lengths. Advantage can be taken of this technique in establishing a schedule of equivalence to relate the effects of explosive charges to the impacts which they are to simulate.

7. Geometry of the rear surface of a target (hence, of a shielding material) may significantly influence the damage sustained by the target.

REFERENCES

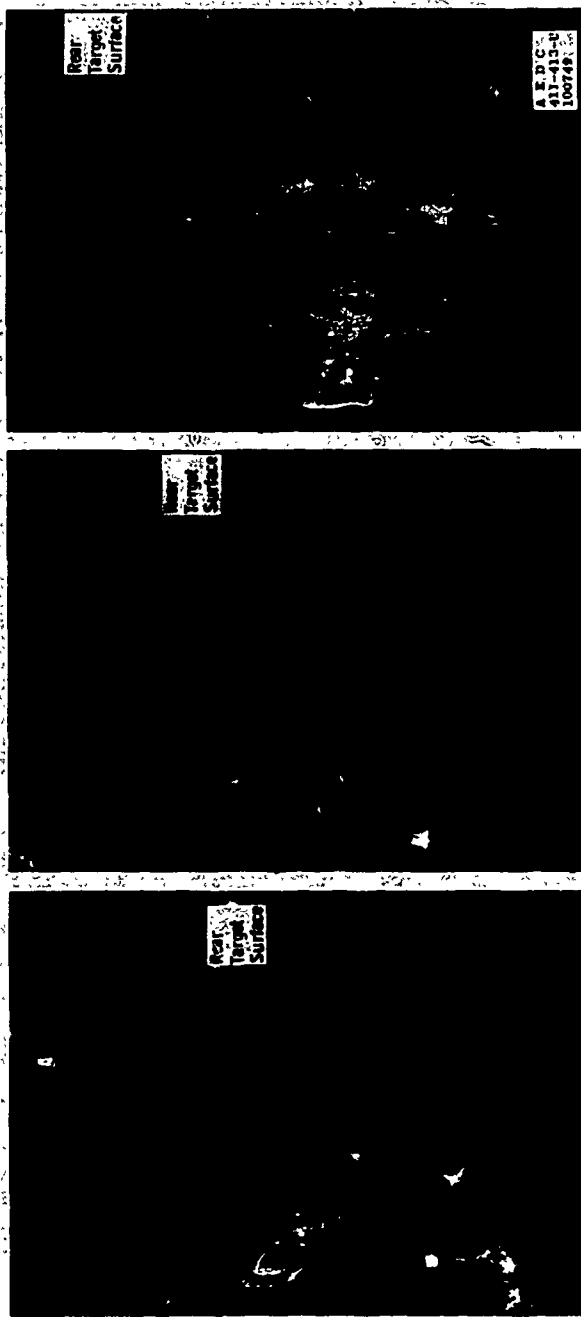
1. Nysmith, C. Robert and Summers, James L. "Preliminary Investigation of Impact on Multiple-Sheet Structures and an Evaluation of the Meteoroid Hazard to Space Vehicles." NASA Technical Note D-1039, September 1961, p. 9.
2. Duberg, John E. "The Meteoroid Hazard of the Environment of a Satellite." NASA Technical Note D-1248, May 1962, p. 3.
3. Kinslow, Ray. "Properties of Spherical Stress Waves Produced by Hypervelocity Impact." AEDC-TDR-63-197, October 1963, p. 11.
4. Kolsky, H. Stress Waves in Solids. Oxford University Press, London, 1953, p. 194.
5. Cook, M. A., Keyes, R. T., and Ursenbach, W. O. "Measurements of Detonation Pressure." Journal of Applied Physics, Vol. 33, No. 12, December 1962, p. 3417.
6. Keller, Donald V. and Trulio, John G. "Mechanism of Spall in Lucite." Journal of Applied Physics, Vol. 34, No. 1, January 1963, p. 175.
7. Rinehart, John S. "On Fracture Caused by Explosions and Impacts." Quarterly of the Colorado School of Mines, Vol. 55, No. 4, October 1960, p. 9.



A E D C
62-220-U
100748

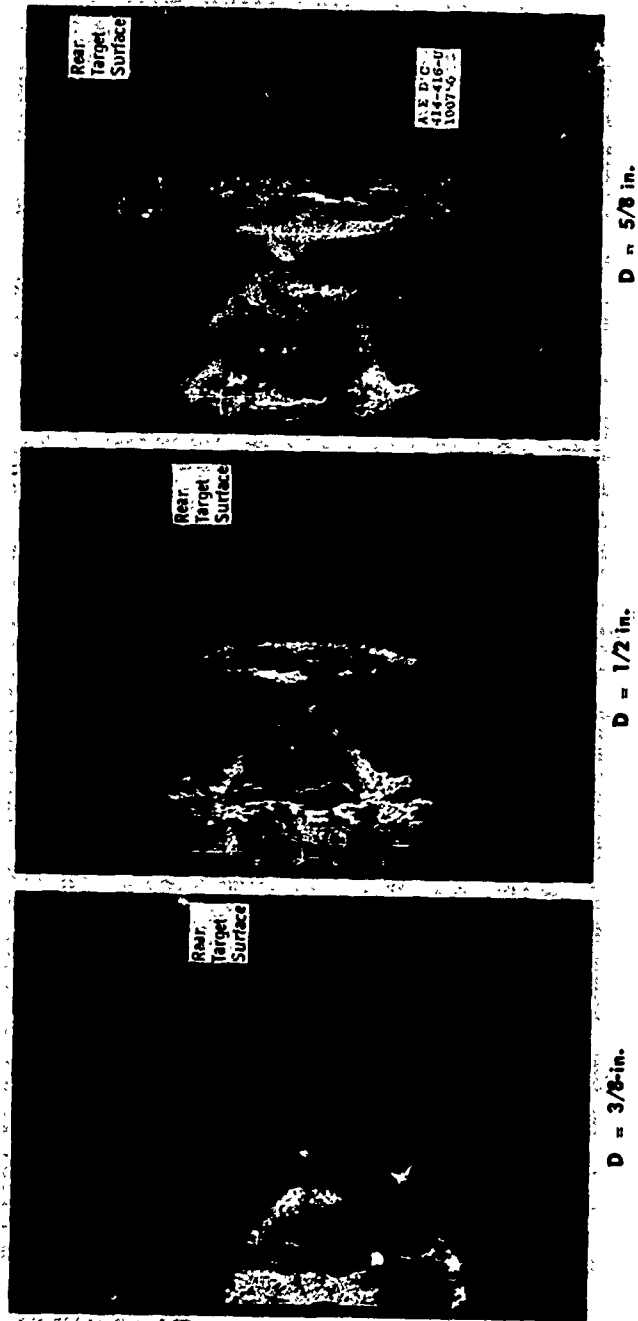
2-in. Lucite Target, 30-cal x 0.15-in. Lexan Projectile,
Projectile Velocity = 21,800 ft/sec

Fig. 1 Hypervelocity Impact of Transparent Target



2.0-in. Lucite Targets Impacted
by 30-cal x 0.15-in. Lexan Projectiles

Fig. 2 Fractures Produced by Hypervelocity Impact



Holes of 0.281-in. diameter were drilled in the faces of large 2-in.-thick Lucite blocks. Aluminum hemispheres of 0.25-in. diameter (rivet heads) were placed in each hole. Number 8 Hercules Powder Co. Blasting Caps were inserted in each hole and fired.

Fig. 3 Fractures Produced by Exploding Blasting Caps

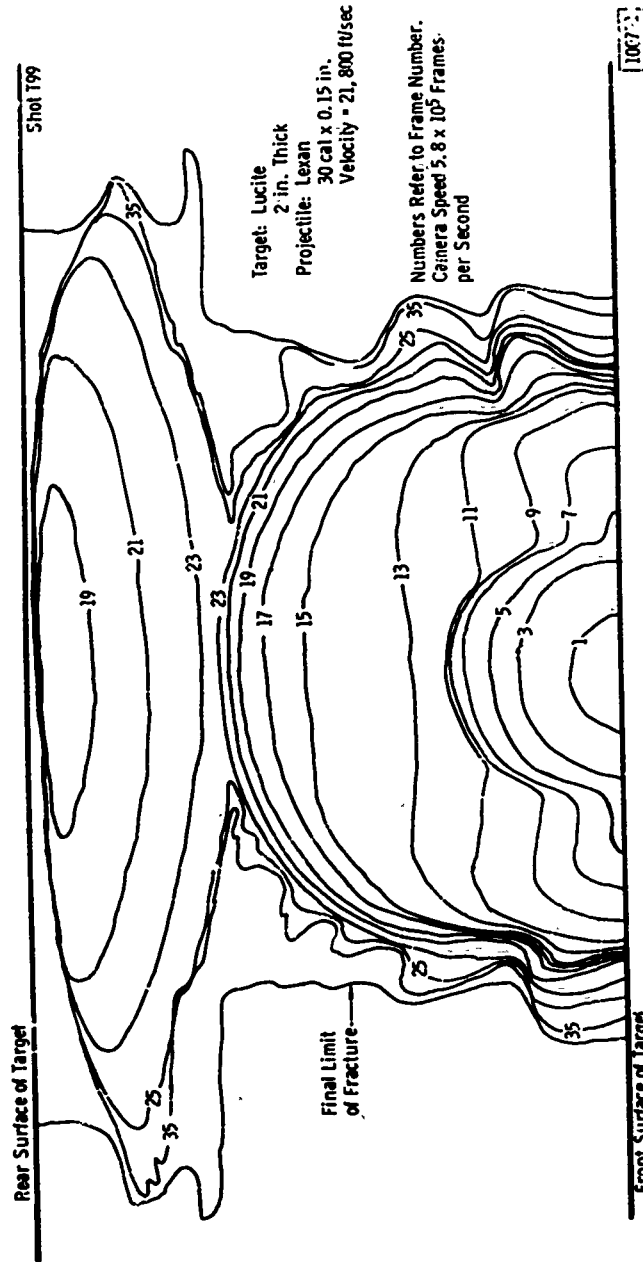
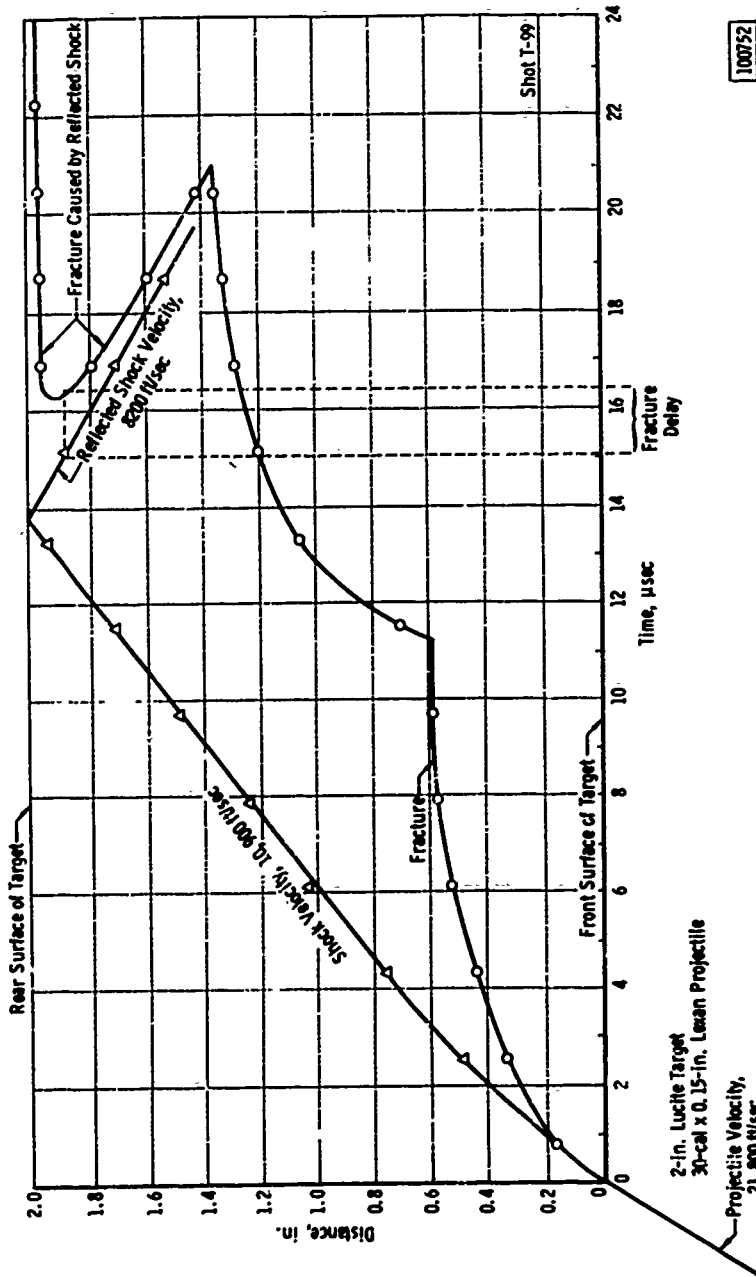


Fig. 4 Fracture Formation (T99)



100752

Fig. 5 Stress Waves and Fracture (199)

2-in. Lucite Target
 30-cal x 0.15-in. Leman Projectile
 Projectile Velocity,
 21, 900 ft/sec



Rear View



Edge View

Sectioned 2-in. Lucite Target
30-cal x 0.15-in. Lexan Projectile
Projectile Velocity = 21,800 ft/sec

Fig. 6 Sector of Fractured Target (T99)

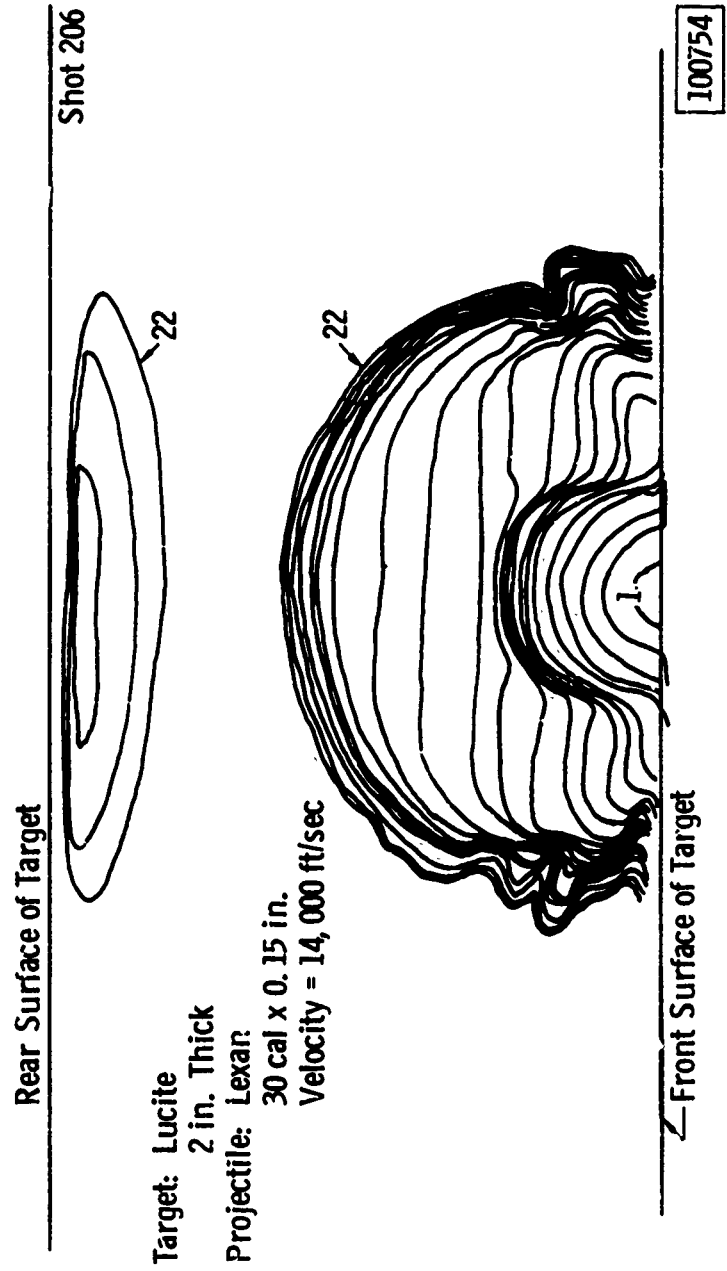


Fig. 7 Fracture Formation (206)



2-in. Lucite Target Impacted by a
30-cal x 0.15-in. Lexan Projectile
at a Velocity of 17,600 ft/sec

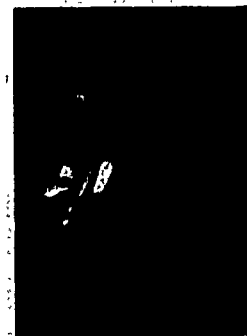
Fig. 8 Section of Fractured Target



Isochromatics



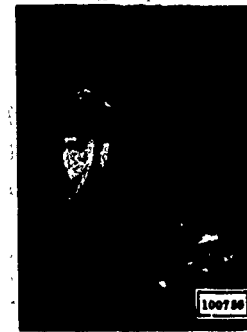
0-deg Isoclinic



15-deg Isoclinic



30-deg Isoclinic



45-deg Isoclinic

Fig. 9 Residual Stresses in Target

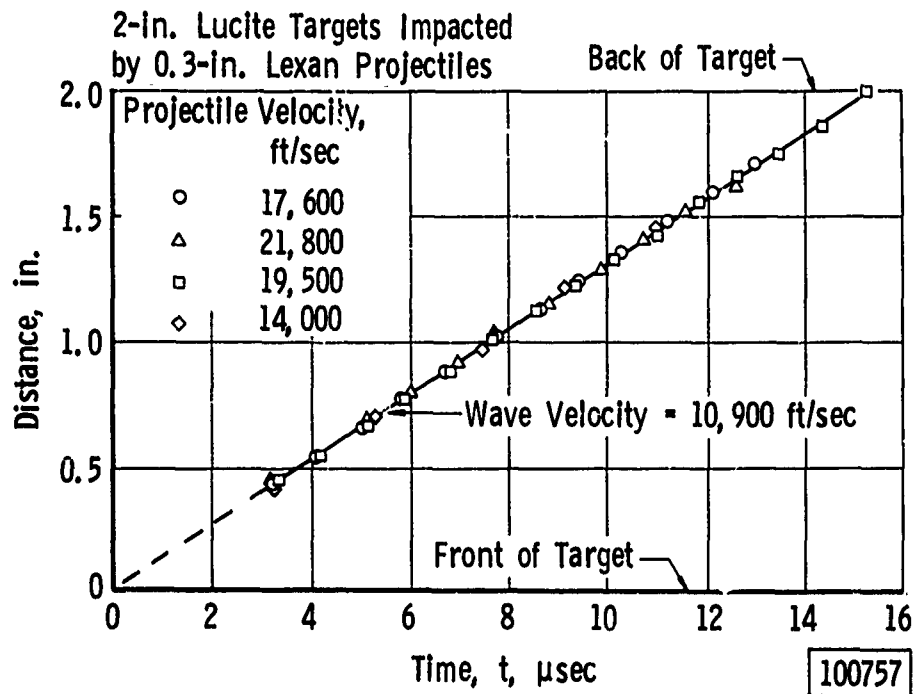


Fig. 10 Pulse Velocity for Various Impact Velocities

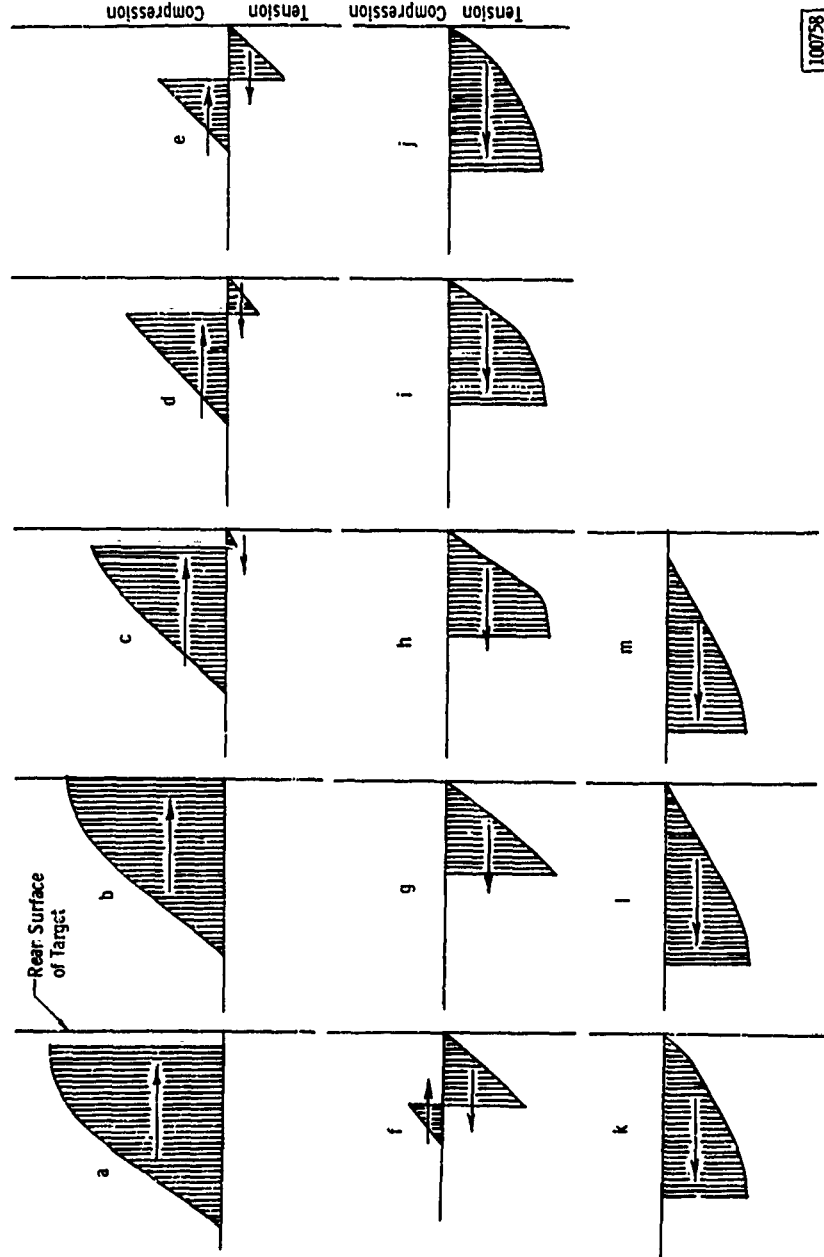
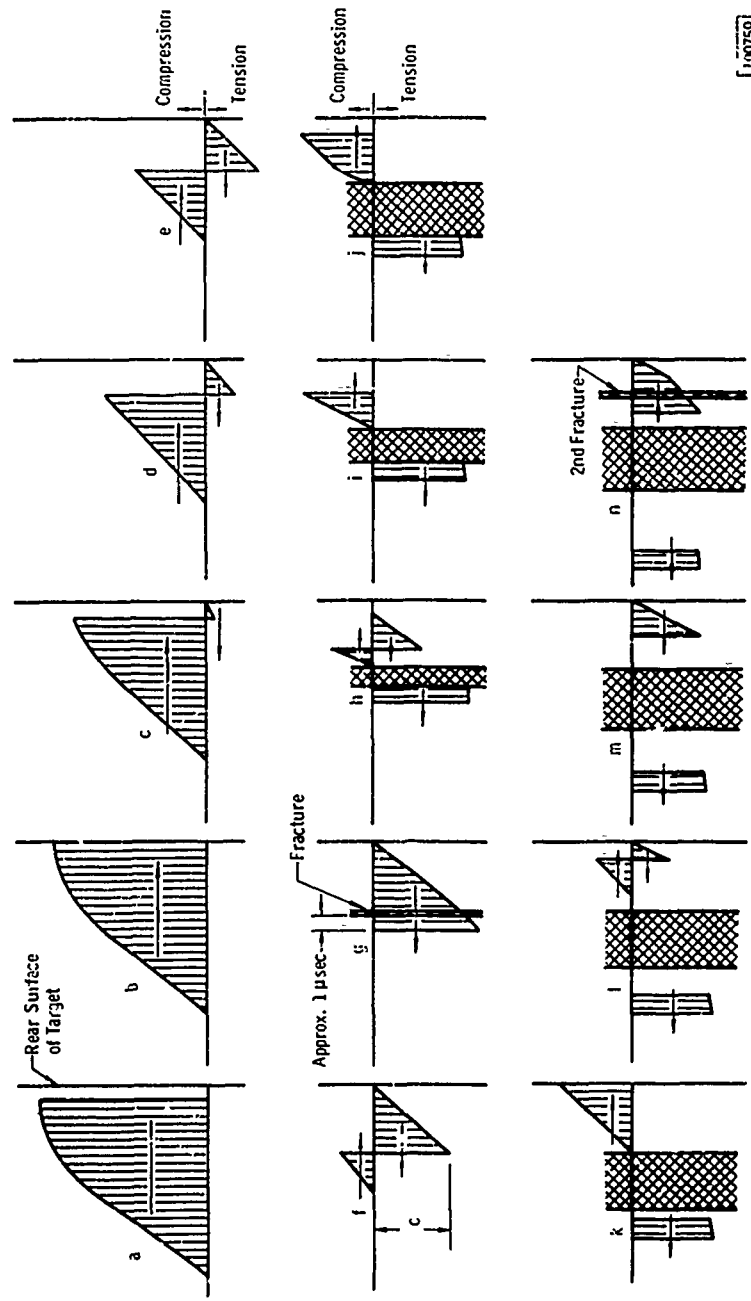


Fig. 11 Development of Radial Tensile Stress Caused by Reflected Pulse



190759

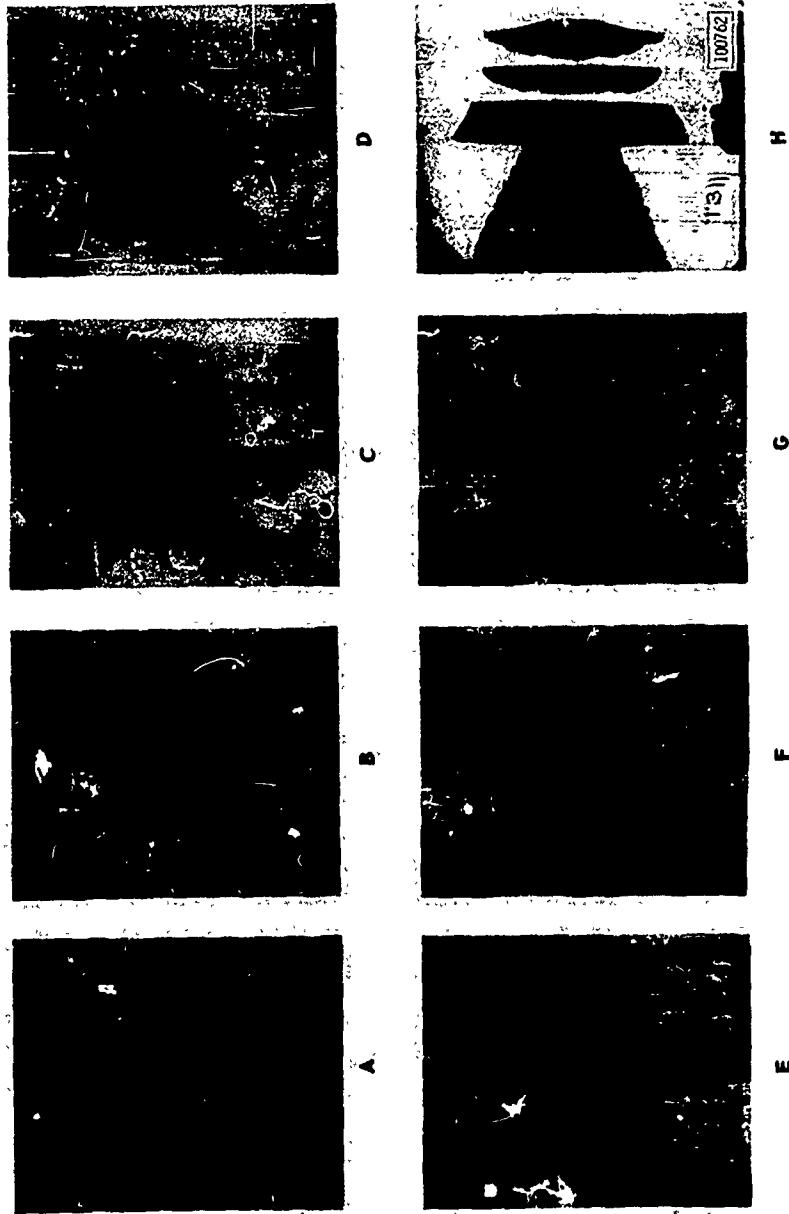
Fig. 12 Mechanics of Fracture Caused by Reflected Pulse



Fig. 13 Photograph of Reflected Pulse Front Moving Ahead of the Fracture



Fig. 14 Example of Secondary Fracture



Target: Three Sheets of 0.75-in. Laminated Plastic
Projectile: 30-cal x 0.15-in. Lexan
Projectile Velocity: 21,100 ft/sec

Fig. 15 Impact of Laminated Target

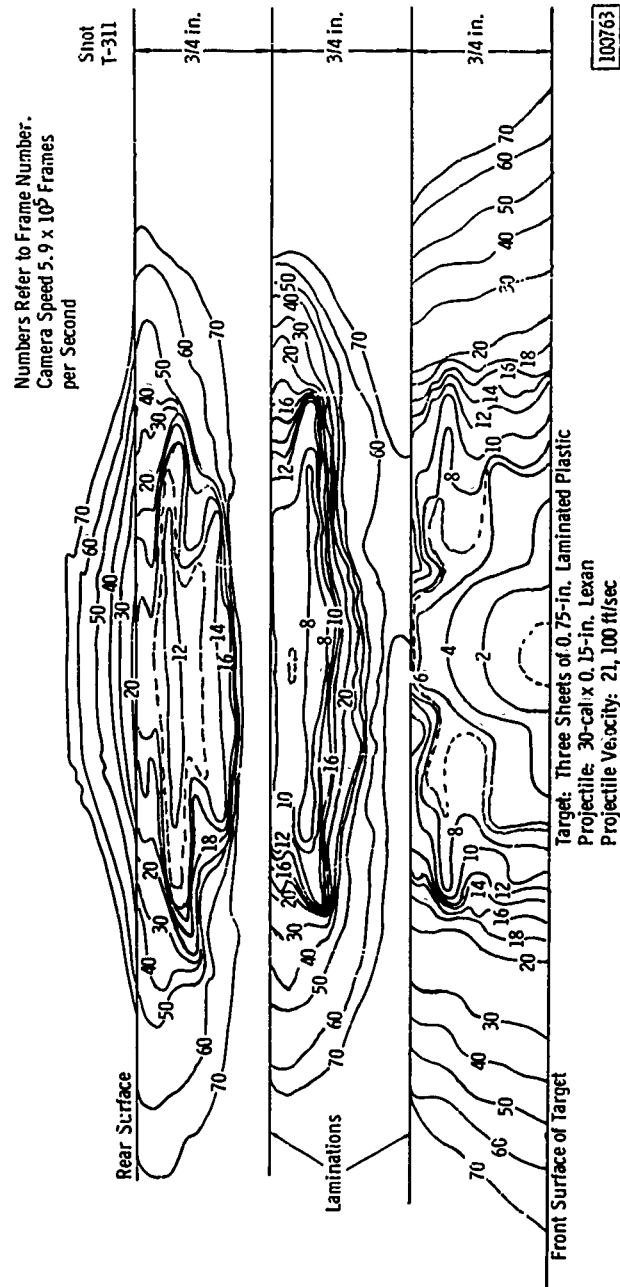
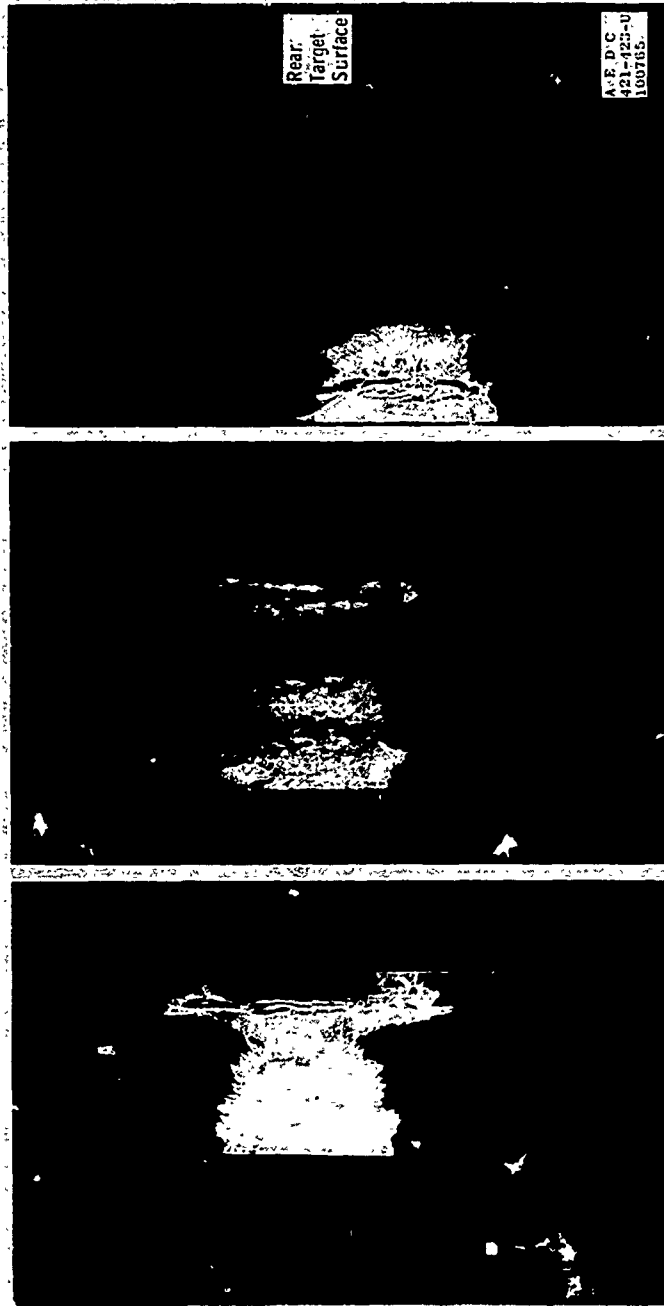


Fig. 16 Fracture Formation in Laminated Target (T311)



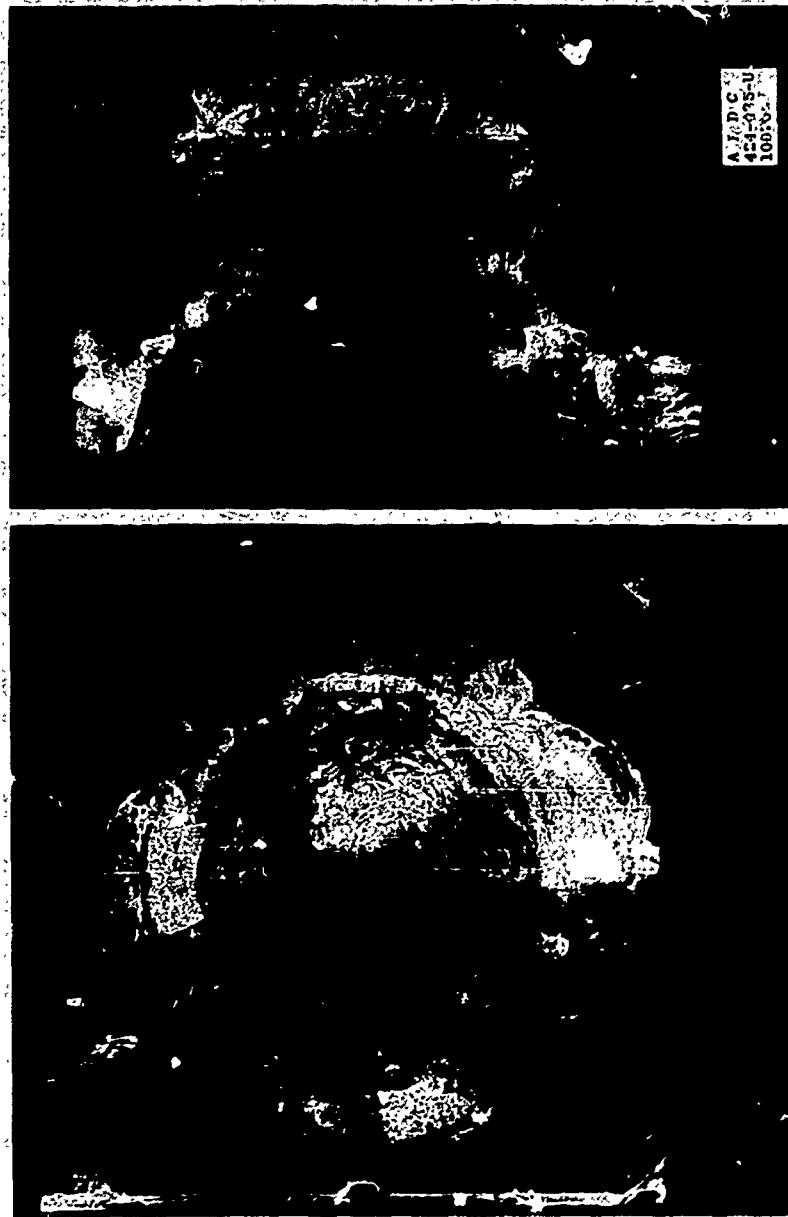
T = 1.50 in.

T = 1.25 in.

T = 1.00 in.

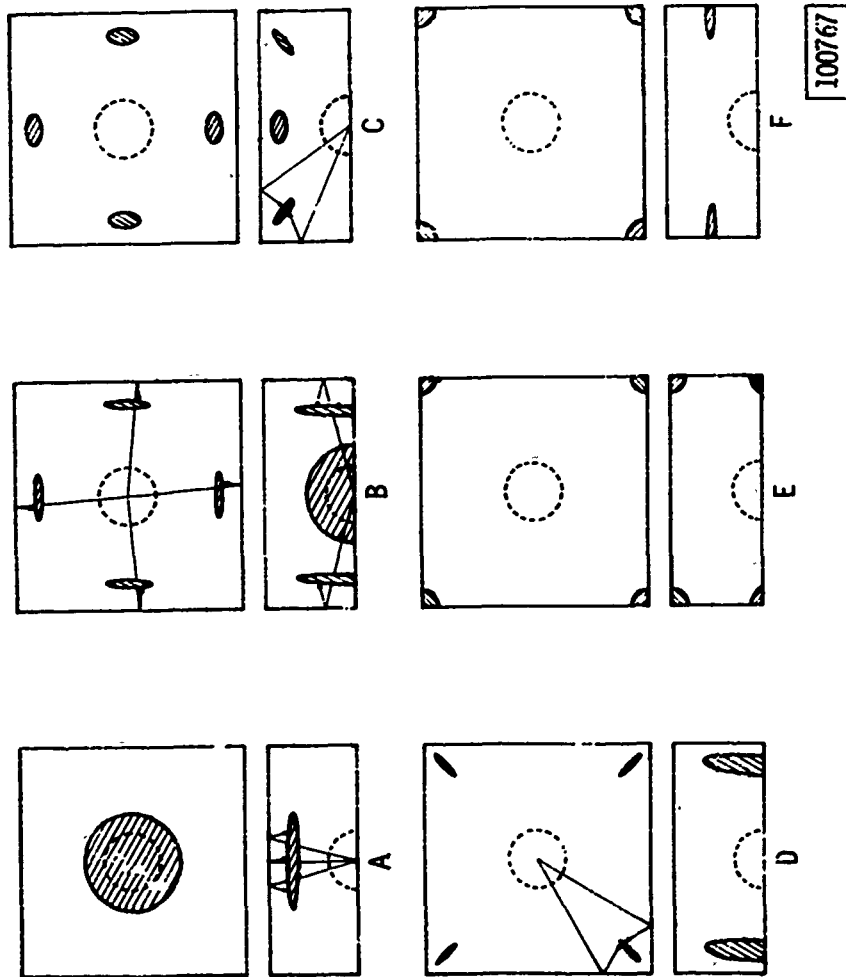
Fractures Produced by Exploding E-94 du Pent
Blasting Caps Inserted in 0.25- x 0.25-in.
Cylindrical Holes in Face of Lucite Blocks

Fig. 18 Effect of Target Thickness



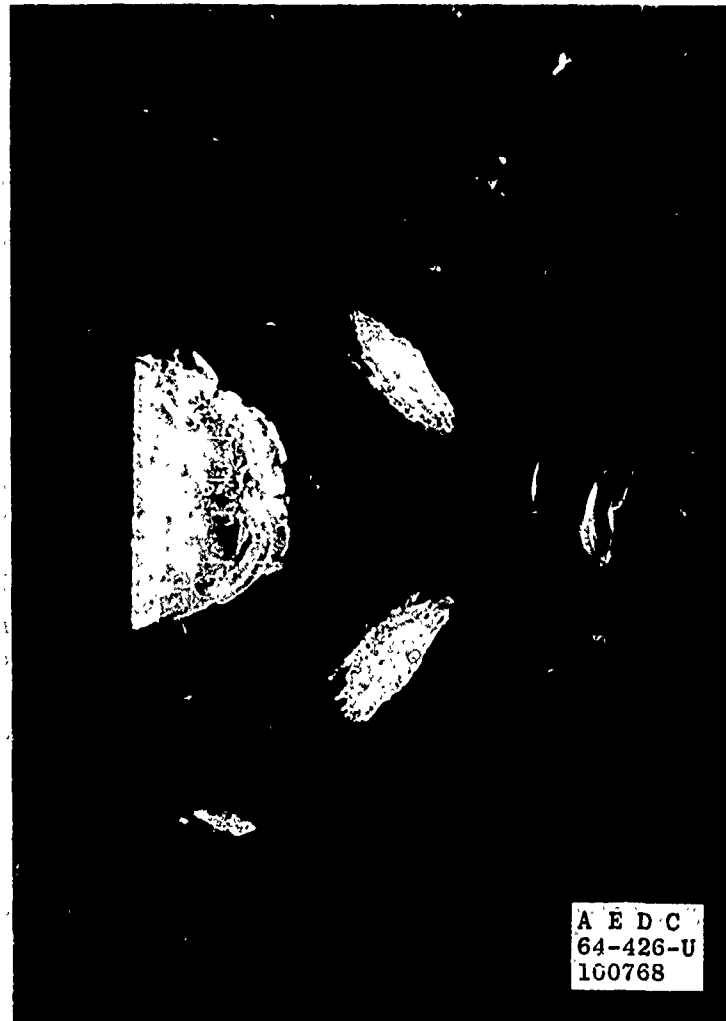
Two Views of a 4- x 4- x 2-in.
Lucite Block Fractured by an Exploding
Blasting Cap

Fig. 19 Fractures in Targets Having Small Lateral Dimensions



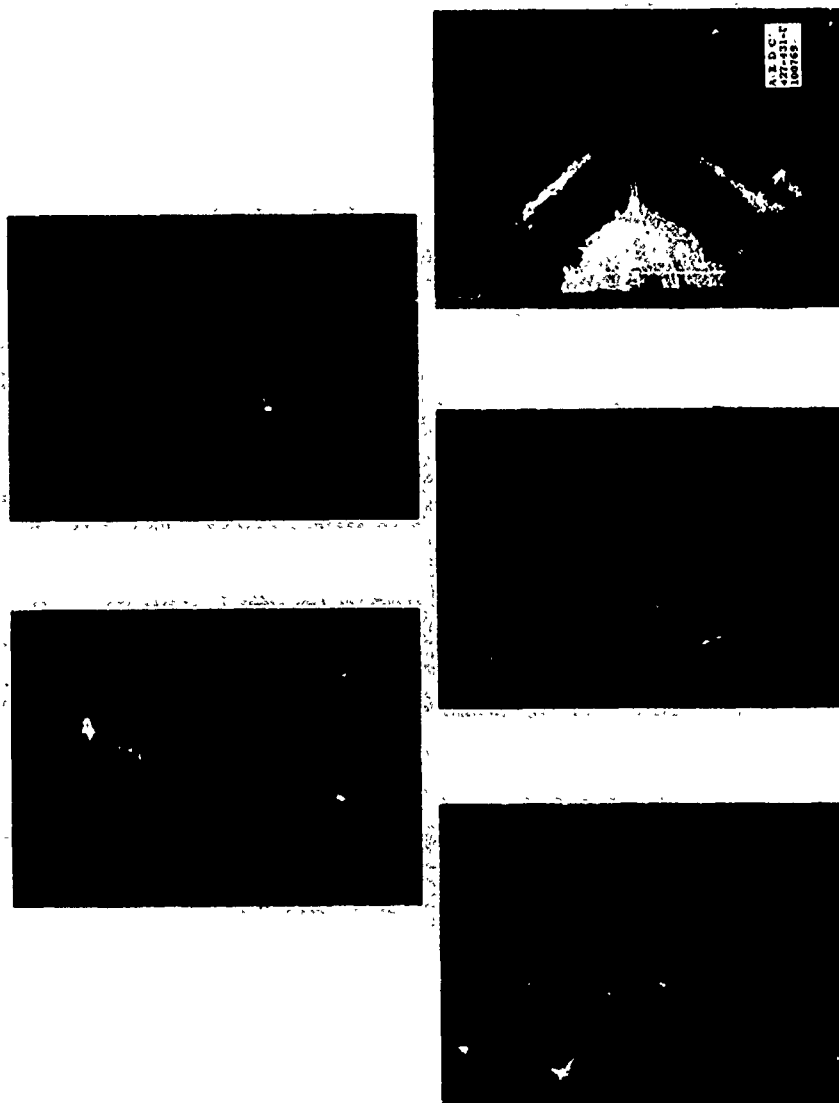
100767

Fig. 20 Mechanics of Fracturing



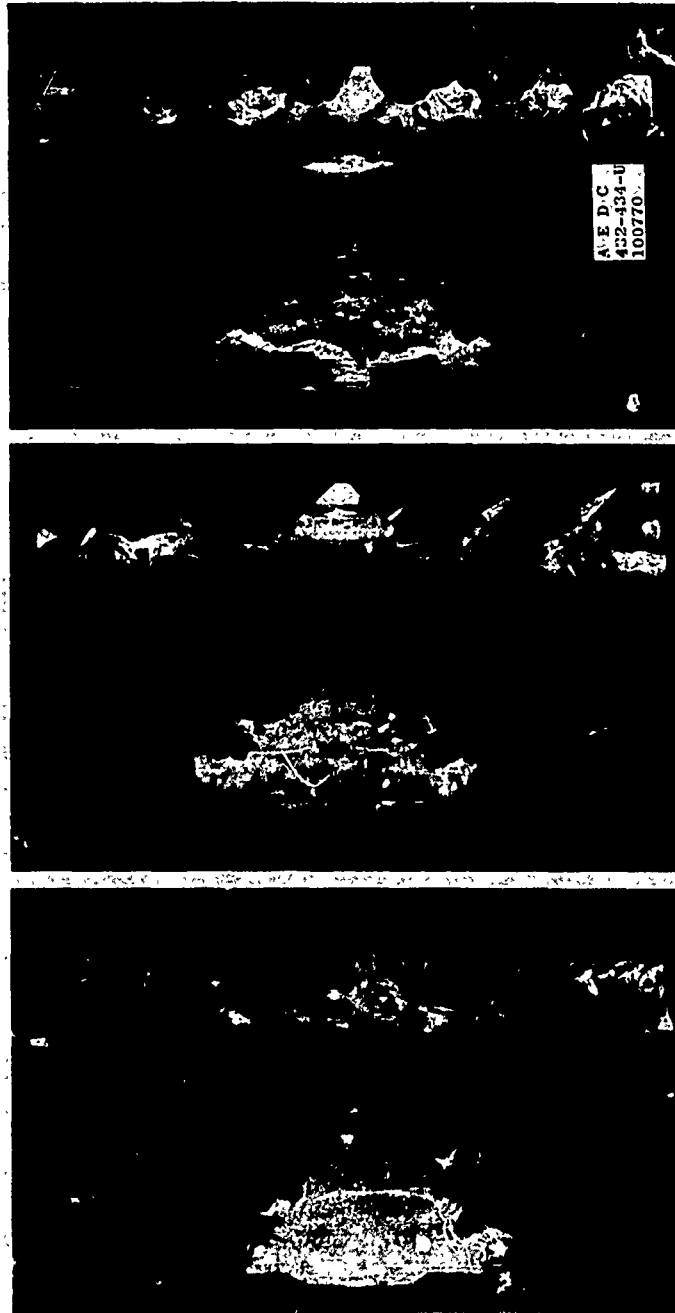
Approximately One-Half of a 4- x 4- x 2-in. Lucite Block
Fractured by a Blasting Cap Exploding at the Center of
the Hypotenuse.

Fig. 21 Fractures in a Triangular Target



Fractures produced by exploding blasting caps. The surfaces from which the pressure pulses were reflected were all of equal distance from the point of the explosions.

Fig. 22 Fractures in Target of Various Geometrical Shapes



C

B

A

Lucite Blocks 4 x 4 x 2 in.
Fractures Produced by Exploding Blasting Caps.

Fig. 23 Effect of Rear Surface Conditions

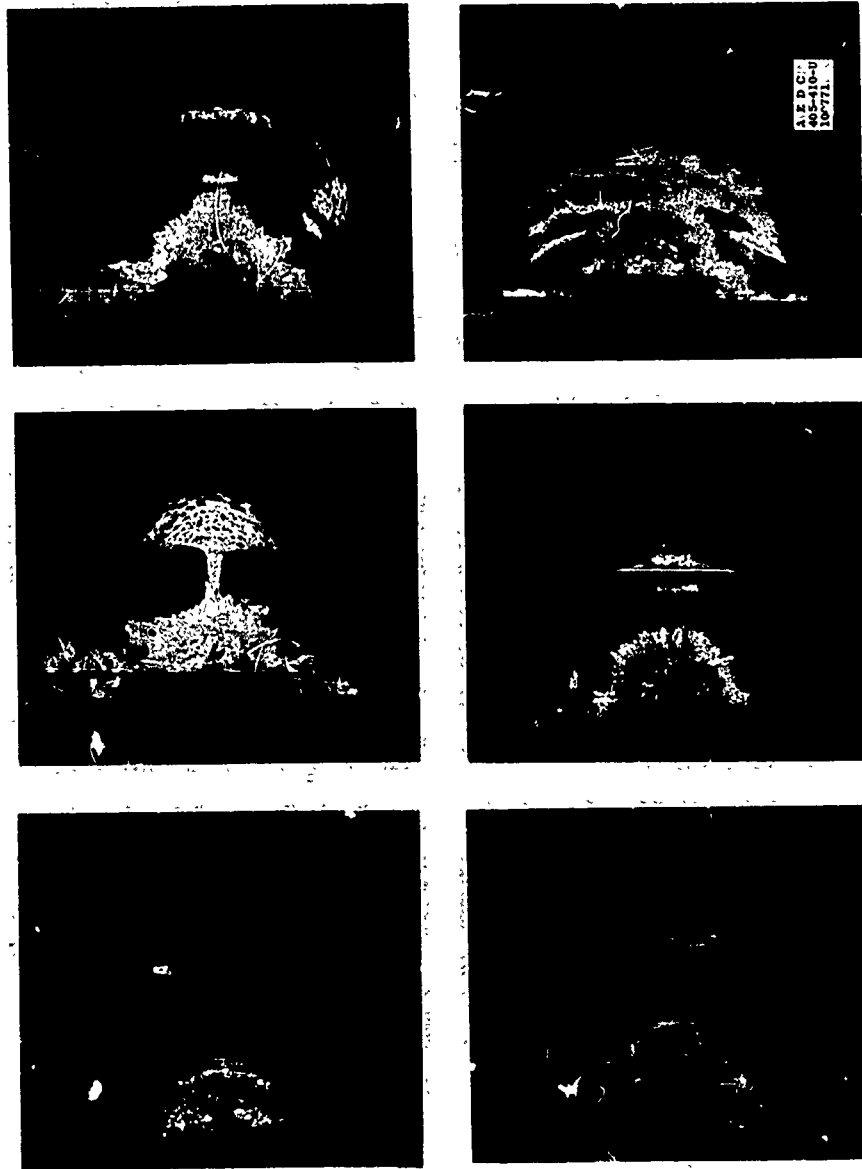
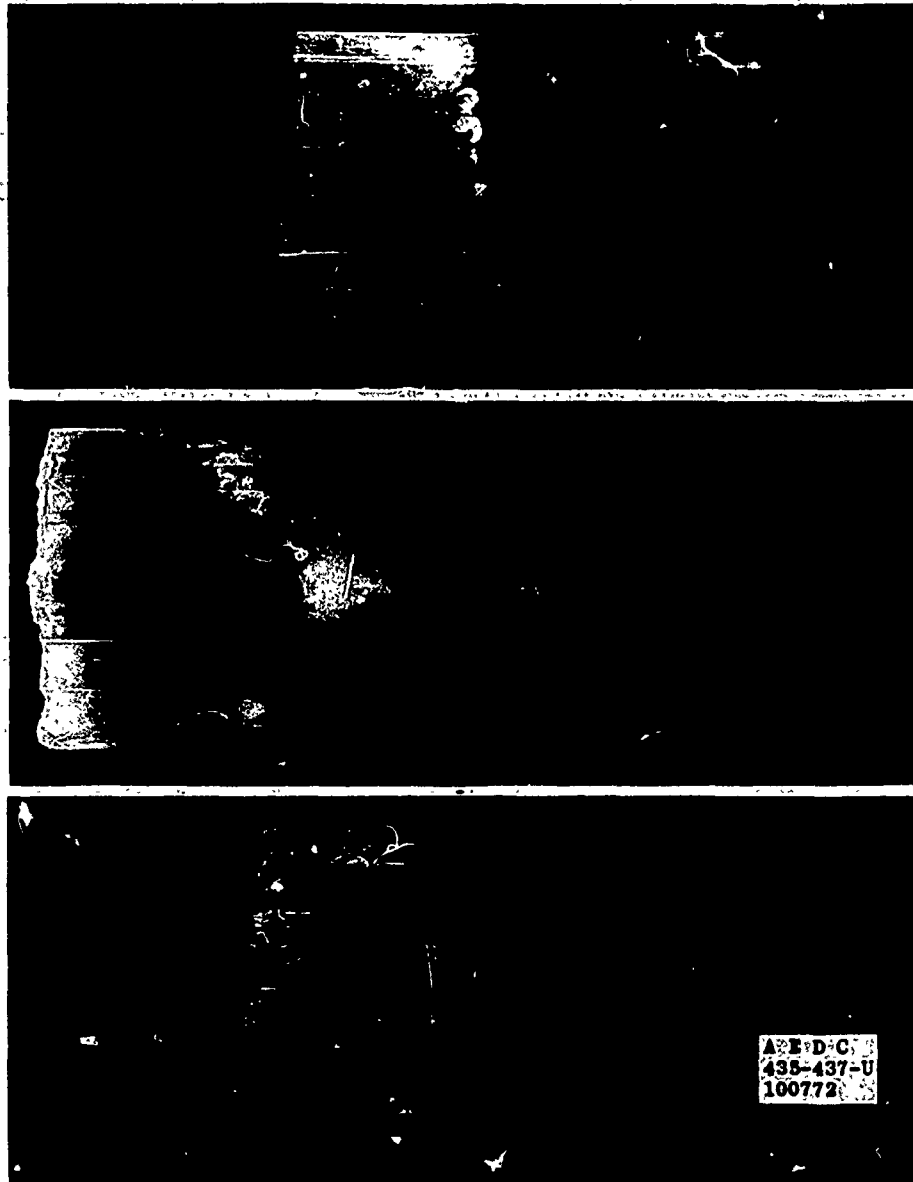
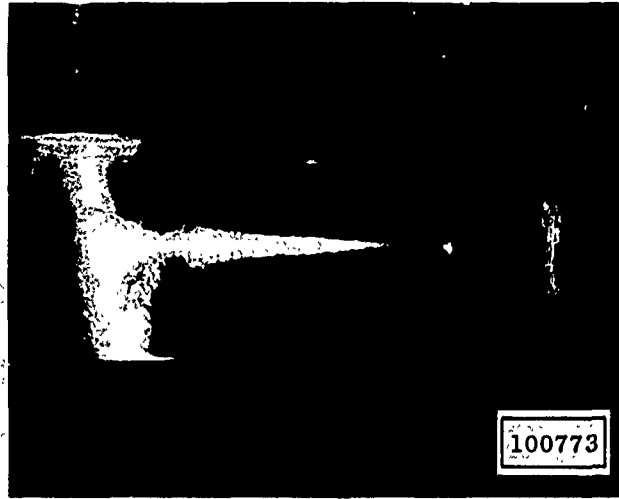


Fig-24 Fractures Caused by Reflections from Curved Surfaces



Fractures Produced by Exploding Blasting Caps at the Ends of Long Rods Having Diameters of 1.25 in.

Fig. 25 Fracture Along Axes of Long Cylindrical Rods

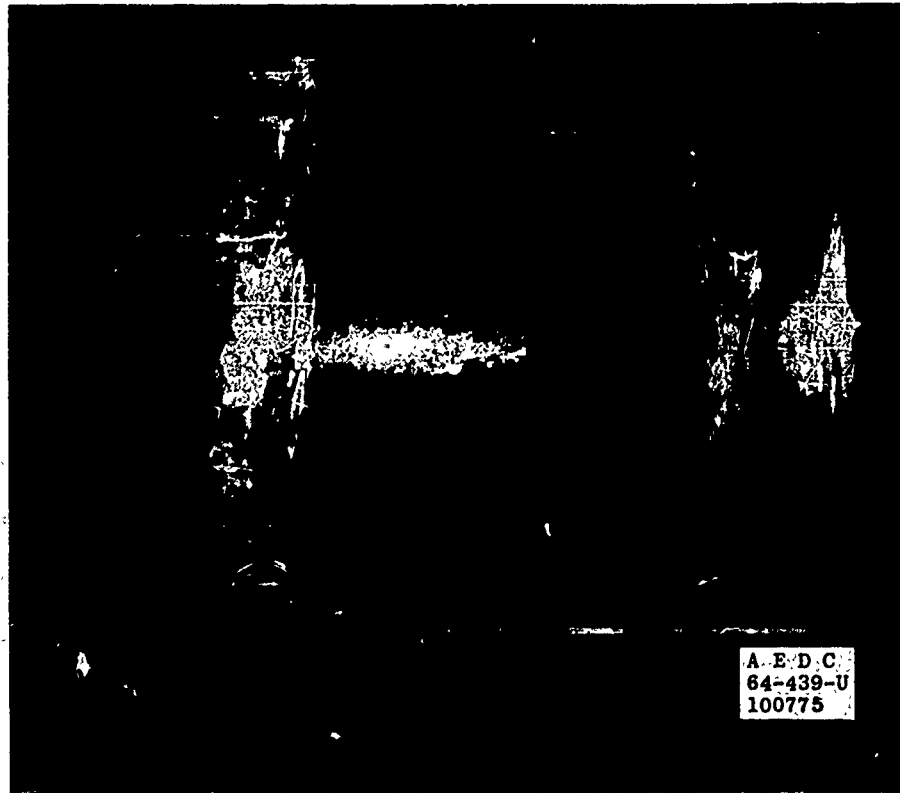


Lucite Rod 1.25 in. Diameter x 3.5 in. Long

Fig. 26 Fractures Along Axis and at End
of a Cylindrical Rod

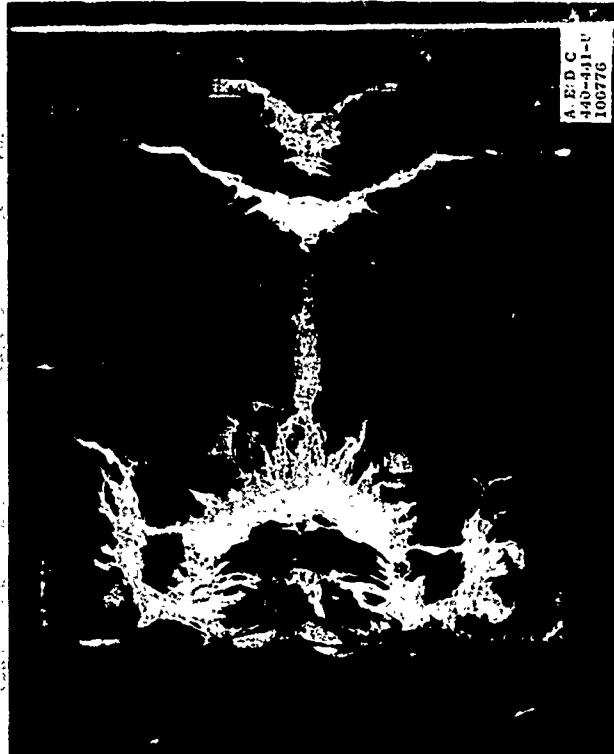


Fig. 27 Transverse Fracture of a Cylindrical Rod

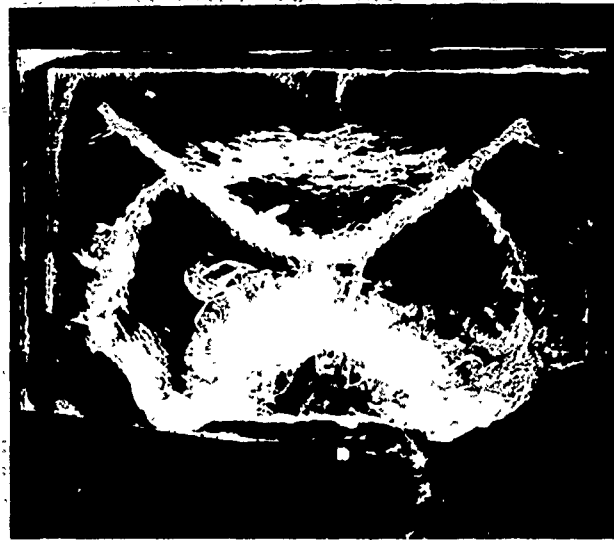


Lucite Cylinder 2.5 in. Diameter x 3.25 in. Long

Fig. 28 Fractures in a Short Cylinder

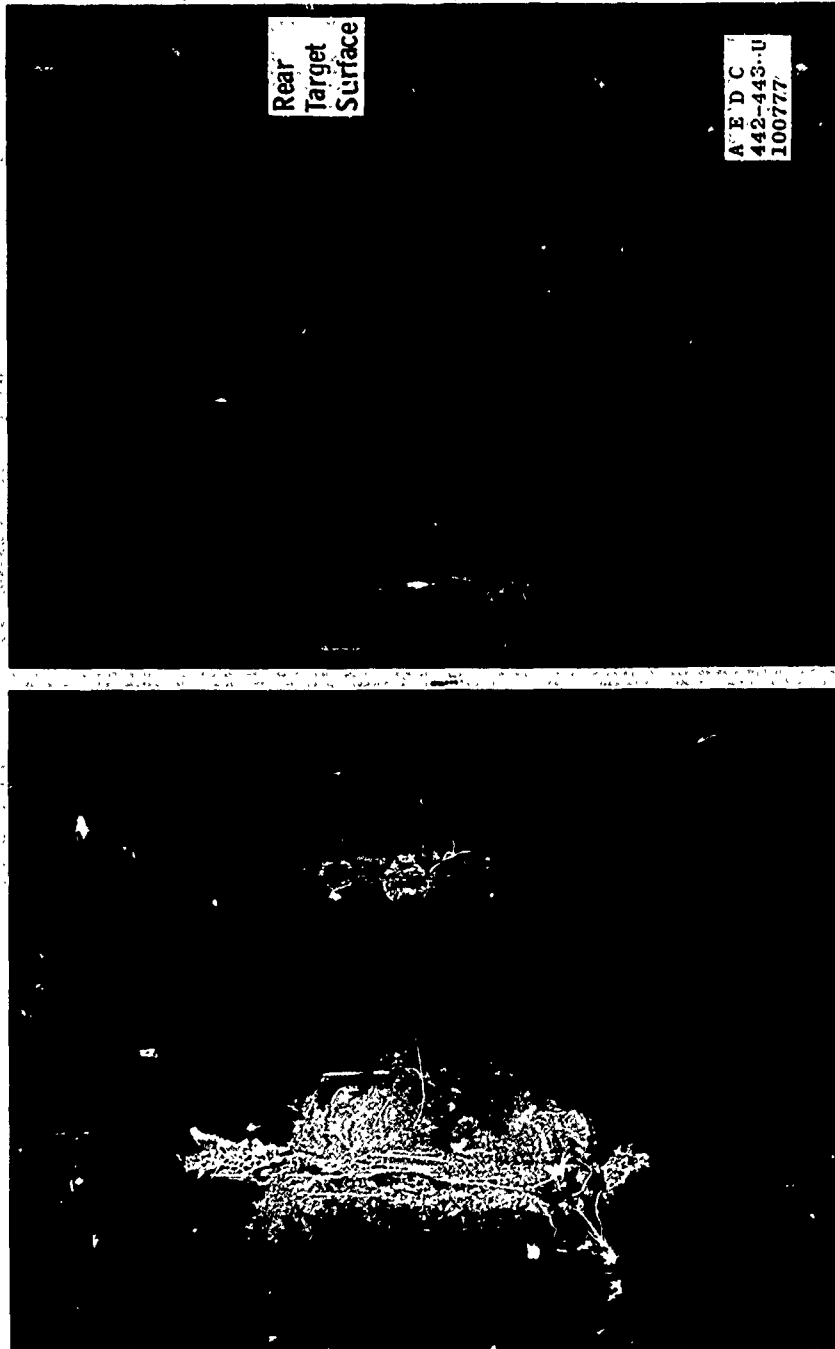


Cylinder 2.5 in. Diameter x 1.5 in. Long



Cylinder 2.5 in. Diameter x 2.5 in. Long

Fig. 29 Sections of Fractured Cylinders



B. Target Temperature, 70°C

A. Target Temperature, 0°C

Fig. 30 Effect of Target Temperature